

SEMICONDUCTOR HETEROSTRUCTURE WEAK LINKS FOR JOSEPHSON AND SUPERCONDUCTING FET APPLICATIONS

A.W. Kleinsasser, T.N. Jackson, G.D. Pettit, H. Schmid, J.M. Woodall, and D.P. Kern
 IBM Thomas J. Watson Research Center
 P.O. Box 218, Yorktown Heights, NY 10598

Abstract

Superconductor-normal-superconductor (SNS) weak links using a semiconductor as the normal region are of interest for applications in high frequency Josephson devices and in superconducting field effect transistors. Recently, there has been a revival of interest in materials such as InAs which, in principle, allow true SNS structures without tunneling (Schottky) barriers at the electrodes. In this paper we discuss the requirements for semiconductor SNS Josephson and FET devices and describe the fabrication and characterization of planar SNS weak links in which the normal region is InAs, which is part of a heterostructure consisting of a thin (100 nm) layer of n-InAs grown on undoped GaAs. Nb electrodes defined by electron beam lithography have been made with spacings as small as 260 nm. Preliminary measurements indicate that the devices have good electrical behavior which is well explained by SNS weak link theory, using coherence lengths calculated from measured material parameters. These weak links can be the basis for superconducting FET devices, and have the significant advantage of allowing simple device isolation compared with bulk InAs, which was used in earlier work.

IntroductionSemiconductor-Coupled Weak Links

Superconductor-normal-superconductor (SNS) weak links are of interest for high frequency applications of the Josephson effect [1], primarily because of their low capacitance compared with tunnel junctions. In contrast with superconducting microbridges, the product of critical current and normal resistance ($I_C R_N$) depends only on the superconducting properties of the banks, not those of the bridge. Because of difficulties in fabricating high T_C tunnel junctions, SNS weak links may be the most promising Josephson devices for applications at temperatures above 10-15 K [2], and operation of SQUIDS based on SNS devices in this range has been demonstrated [3]. Semiconductors, rather than metals, are of significant interest as weak link materials [4] because useful device impedances (tens to hundreds of ohms) are easily possible.

Relatively little work has been done on semiconductor-coupled SNS devices. Although significant effort has been devoted to Si-based devices [4-6], the Schottky barriers which exist at Si (and most other semiconductor)-metal interfaces, result in a SINIS (rather than SNS) structure. Here I (insulator) denotes the tunnel barrier which is present between the link and electrode materials, and which evidently has a major effect the device behavior [5,7]. In certain semiconductors, such as InAs and InSb, the Fermi level is pinned in the conduction band at metal interfaces (and other surfaces). Thus, a Schottky barrier-free contact forms between metals and n-InAs, and an electron-rich inversion layer with no barrier between itself and the metal forms at metal/p-InAs interfaces. Weak links based upon these materials should have true SNS, rather than SINIS, character. Attempts to form Josephson weak links on InAs were made a number of years ago, and suggestive results indicating superconducting interactions between the electrodes were obtained [8]. However, the first demonstration of Josephson behavior in such weak links was made only recently [9].

Josephson FETs

SNS weak links are the basis for a superconducting field effect transistor, first proposed a number of years ago [10,11], in which the strength of the Josephson coupling (i.e. the supercurrent) is controlled by adjusting the carrier concentration in the link (or FET channel) via a gate. Such devices have been demonstrated recently on InAs [12,13] and on Si [6,14]. In the former case the devices appear to act as SNS weak links, but response to a gate voltage is poor; several volts applied to the gate of a Nb/p-InAs/Nb device

changes the critical current or device resistance by considerably less than a factor of 2. Evidently the strong pinning of the Fermi level in the conduction band at interfaces not only gives barrier-free contacts, but also makes it difficult to vary the surface potential with an electric field. Also, the presence of a highly conductive layer over the entire surface of an InAs wafer makes device isolation difficult. On the positive side, the absence of Schottky barriers, the low effective mass, and the high carrier mobility in InAs allow significantly larger device lengths and/or lower dopings for InAs compared with Si (for a given Josephson critical current). In the case of Si the SNS weak link model is inadequate, presumably due to Schottky barriers and a SINIS structure. The device behavior is not well understood; in particular the gate response of the critical current is far larger than expected, although the corresponding change in the normal resistance is negligible.

In the following sections, some of the requirements for semiconductor SNS weak link and FET devices are discussed. We also describe some recent results on a new weak link structure which allows device isolation and appears promising for both weak link and FET applications.

Device RequirementsSemiconductor-Coupled Weak Links

Metallic SNS weak links tend to have low impedances, due to the low resistivity of the bridge material. For example, a 10 nm thick film of 10 $\mu\text{m-cm}$ material has a sheet resistance of 10 Ω/\square . Device lengths are constrained to be less than a few hundred nanometers [15], so that a 50 Ω device must have a width of order 100 nm, a formidable lithographic challenge. Thus high resistivity is very important, and semiconductors and semimetals become obvious candidates for bridge materials.

The critical current of an SNS weak link depends strongly on its length, the scale of which is set by the normal metal coherence length, ξ_N . For an n-type semiconductor [16],

$$\xi_N(T) = (\hbar^3 \mu / 6\pi m^* e k_B T)^{1/2} (3\pi^2 n)^{1/3} \quad (1)$$

where μ , m^* , and n are the electron mobility, effective mass, and density. The $I_C R_N$ product is the most important figure of merit for a Josephson device. Likharev obtained, for an SNS weak link,

$$I_C R_N = \frac{4\Delta^2(T)}{\pi e k_B T} \frac{L}{\xi_N} e^{-L/\xi_N}, \quad (2)$$

where Δ is the energy gap in the superconducting electrodes, L is the link length, and R_N is the normal state resistance [17]. Equation 2 applies to long bridges ($L \gg \xi_N$), and is valid near T_C . Seto and van Duizer [16] had earlier obtained an equivalent functional dependence for the critical current of SINIS semiconductor weak links on temperature, length, and doping under certain conditions, although they were not able to predict the magnitude of $I_C R_N$. These results are used by most authors in discussing both SNS and SINIS semiconductor weak link behavior [4,6,9]. For short bridges ($L \ll \xi_N$), also near T_C ,

$$I_C R_N = \frac{\pi \Delta^2(T)}{4 e k_B T}. \quad (3)$$

As the temperature is lowered, the effective bridge length $L/\xi_N(T)$ is reduced and $I_C R_N$ saturates at roughly the Ambegaokar-Baratoff result for tunnel junctions ($\pi \Delta(0)/2e$) when L is less than approximately $\xi_N(T_C)$. Equations (2) and (3) lose validity at low temperatures, and further lowering of the temperature does not significantly increase the $I_C R_N$ product, even for extremely short bridges, even though $\xi_N(T) \propto T^{-1/2}$, making the effective bridge length at low operating temperatures quite small. So $L/\xi_N(T_C) \sim 0.5-1$ is optimal [17], and shorter bridges are not really any better. The variation of $I_C R_N$ with temperature is significant unless the temperature is reduced to

$\approx 0.2T_C$, below which $I_C R_N$ is fairly constant [17]. For many applications, a large temperature variation is unacceptable, so that operating temperatures in the 4 K range would be required, even with an electrode T_C of 20 K.

Device length L should be as long as possible, to ease fabrication and to give a large resistance (in many applications tens or hundreds of ohms is a desirable figure), but the exponential decrease in $I_C R_N$ with L dictates that the optimum length is $L \sim \xi_N(T_C)$, so that $I_C R_N \sim \Delta/e$. From Equation 1, high mobility, low effective mass, and high carrier concentration imply large coherence length and therefore allow long devices.

As an example of what can be achieved with semiconductor SNS weak links, consider 10 nm thick InAs bridges of length $L \sim \xi_N$ and widths 1 and 10 μm (such devices will have optimal $I_C R_N$ products at low temperatures, as high as ~ 1.5 mV for Nb electrodes). Figure 1 is a plot of device length and resistance as functions of carrier concentration at 4.2 K (a fixed mobility of 10^4 $\text{cm}^2/\text{V}\cdot\text{s}$ is assumed). Device lengths of up to ~ 1 μm are possible with reasonable dopings. However, in this example, a resistance in the 10-100 Ω range requires that the device length be in the 200-600 (60-200) nm range for 1 (10) μm width, with appropriate doping. High impedance devices with metal bridges would have to be much narrower [15]. Of course smaller widths could be used to achieve larger resistances with semiconductor bridges, allowing longer lengths, but it should be noted that it is significantly easier to fabricate devices with one sub-micrometer dimension (through use of edge or sidewall techniques) than two. This is a major point in favor of semiconductor-coupled weak link devices.

For a device of optimal length ($L \sim \xi_N$), $R_N \propto \rho \xi_N \propto \mu^{-1/2} n^{-2/3}$. Increasing μ and/or n , in order to increase device length, results in a decrease in device resistance. However, an increase in μ allows n to be reduced proportionally (ρ constant), still resulting in slightly larger values for R_N and ξ_N ($\propto n^{-1/6}$). So far, the bridge has been assumed to be three-dimensional. Extremely high mobilities, and therefore large coherence lengths, can be achieved in two-dimensional electron gases. The 3D InAs layer in the above example was 10 nm thick. For a given value of μ , such a layer with $n = 10^{18}$ cm^{-3} will have the same values of ξ_N and R_N as a 2D layer with a sheet carrier concentration $N_S = 10^{12}$ cm^{-2} . For the 2D layer, $\rho \propto (N_S \mu)^{-1}$ and $\xi_N \propto (N_S \mu)^{1/2}$, so that $R_N \propto \rho \xi_N \propto (N_S \mu)^{-1/2}$. Thus an increase in μ along with a proportional decrease in N_S has no effect on R_N or ξ_N . Low carrier density is of particular interest in the FET devices discussed below.

Josephson FETs

From Equations 1 and 2, the critical current of an SNS weak link can be controlled by varying n . A gate voltage V_G changes the carrier concentration in a narrow surface channel, so that a 2D weak link structure is preferred. For simplicity, we consider a thin 3D layer and assume that $\Delta n = C_G \Delta V_G / e$, so that (1) and (2) can be used to obtain:

$$\frac{dI_C}{dV_G} = \left(\frac{L}{\xi_N} - 1 \right) \frac{C_G I_C}{3en}. \quad (4)$$

A large response requires the lowest carrier concentration consistent with good weak link properties, and the device should work in the range $L/\xi_N > 1$; note that the response becomes poor as $L \rightarrow \xi_N$. Since a large value of ξ_N is

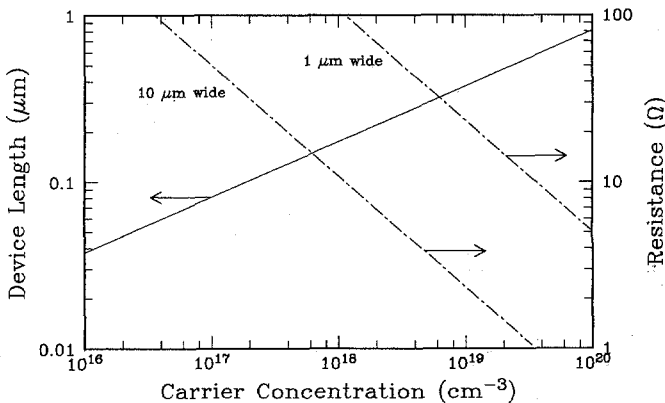


Figure 1: Device length and resistance vs. carrier concentration for n-InAs SNS weak links at 4.2 K, assuming $L \sim \xi_N$. 10 nm bridge thickness and a fixed mobility of 10^4 $\text{cm}^2/\text{V}\cdot\text{s}$ are used.

desirable, mobility should be as large as possible, since this allows smaller carrier densities for given values of ξ_N and R_N .

The Josephson FET has difficulties as a switching device. I_C is exponentially sensitive to changes in n , while R_N changes only linearly. Thus, in switching between zero and finite voltage states, the source-drain voltage drop is likely to be no larger than a few times the $I_C R_N$ product in the superconducting state, a few mV or less. It is difficult to imagine producing significant changes in I_C or R_N without applying gate voltages of at least many tens of mV. Thus the device lacks voltage gain. Although there may be applications for which this is not an issue, it is clear that a truly interesting device (one with voltage gain) must undergo a large change in R_N with changing gate bias, allowing switching out to reasonable voltages (~ 100 mV). This implies a low voltage, but otherwise conventional, FET. Although the technology appropriate for producing Josephson SNS weak link FETs is of interest for such applications, it is not clear that superconductivity will play more than a secondary role in them.

Gate control of the surface potential in the channel region is of fundamental importance in FETs, and is very poor in the InAs devices demonstrated so far [12,13]. The ability to control the conductivity of an InAs (or similar material) layer with a gate is an area which obviously needs experimental attention.

Heterostructure InAs Weak Links

In materials such as InAs and InSb, the pinning of the surface Fermi level in the conduction band allows contacts without Schottky barriers. One major drawback with such materials is that isolation of devices from one another is difficult, due to the presence of a conducting layer over the entire wafer surface. In order to allow simple device isolation, and to allow control of the channel/weak link thickness, we have been exploring the fabrication of Nb/n-InAs/Nb weak links in which the InAs is a thin film, part of an InAs/GaAs heterostructure [18]. These layers are grown on semi-insulating GaAs, allowing simple device isolation by mesa etching. There is a relatively large ($\approx 7\%$) lattice mismatch between GaAs and InAs, however we obtain mirror-like films with only occasional small surface defects. The InAs films can be n-doped with Si over a wide range (3.5×10^{17} to 5.9×10^{19} cm^{-3} has been obtained in the course of this work). Hall mobilities are 5000, 2000, and 1900 $\text{cm}^2/\text{V}\cdot\text{s}$ at 3.5×10^{17} , 3.5×10^{18} , and 3.1×10^{19} cm^{-3} respectively, essentially constant from room to liquid nitrogen temperature. For comparison, in the weak link experiment on bulk n-InAs, mobilities of 16900 and 10000 $\text{cm}^2/\text{V}\cdot\text{s}$ for dopings of 2.5×10^{17} and 2.6×10^{18} cm^{-3} were reported [9].

Several SNS bridges were fabricated on a 100 nm thick $3.5 \times 10^{17} \text{cm}^{-3}$ n-InAs layer. For this doping, the Fermi level is ~ 75 mV into the conduction band in the bulk of the InAs layer. At the Nb-InAs interface the situation is not dramatically different. Thus the electron concentration is more or less uniform throughout the layer; in particular, the electrons are not concentrated in a thin layer at the surface. This is borne out by the fact that the sample doping and measured electron concentration do not differ significantly in our samples. We therefore expect the InAs to behave as a three-dimensional low carrier density thin metal film. The results presented below are consistent with this expectation.

The devices are 25-200 μm wide, with 65 nm thick Nb electrodes spaced 0.26-3 μm apart. Resistances of these bridges are consistent with measured 77 K resistivity of the InAs film and device dimensions, indicating that contact resistance is very small. Supercurrents are observed at 4.2 K in the four shortest devices. Any supercurrents in the longer links were below ≈ 1 μA . The current-voltage characteristics of one link at 4.2 K is shown in Figure 2. The excess current characteristic of SNS weak links was evident in all of the devices. The IV curves are non-hysteretic at 4.2 K. In the shortest link, hysteresis appears when the sample is cooled below 3 K.

As expected, the critical current of our devices is dominated by the increase in coherence length with decreasing temperature (our shortest device is 0.26 μm long, with $L/\xi_N = 2.5$ at 1.4 K, the lowest temperature used). From this measurement, the value $\xi_N(4.2\text{K}) = 0.060$ μm is obtained. Using Equation 1, with the measured values of mobility and carrier density, an effective mass of 0.048 is inferred for InAs. The textbook value [19] is 0.023. However, at a doping level of 3.5×10^{17} cm^{-3} , the Fermi level is well into the conduction band, and the value of the effective mass is larger than it is at the band minimum.

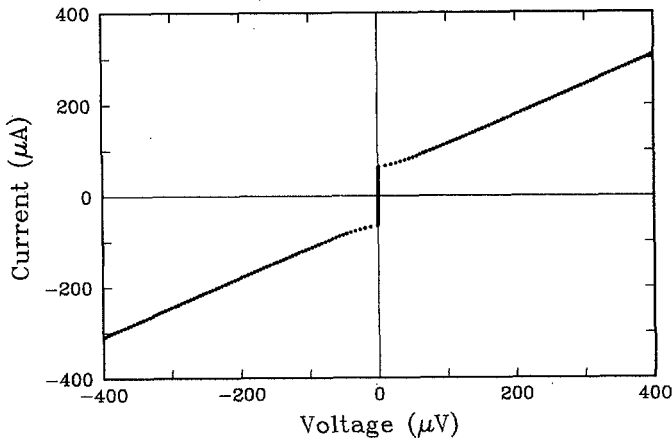


Figure 2: Current-voltage characteristic for an InAs-coupled weak link at 4.2 K.

In Figure 3, device critical current is plotted against measured link length. The solid circles are our data, and the triangles were obtained from Ref. 8 for bulk n-InAs devices with roughly the same doping (the 2 K data from that paper were extrapolated to 4.2 K using the known temperature dependence). The critical currents of our thin InAs layer devices are consistent with the bulk InAs results. Note, however, that the coherence lengths for the bulk sample and our thin InAs sample are different, due to the differing mobilities. The two lines in the figure are included to show consistency with the expected $\exp(-L/\xi_N)$ dependence (only the slopes of the lines are relevant). The values of ξ_N used were $0.144 \mu\text{m}$ for the bulk sample (dashed line) and $0.060 \mu\text{m}$ for our sample (solid line); both numbers are obtained from temperature dependence of the critical current.

Figure 4 is a plot of the $I_C R_N$ product as a function of device length, at 4.2 K. The R_N values are the differential resistances at voltages large enough that the IV's are linear, $\approx 10 \text{ mV}$. The solid curve is the theory of Likharev (Equation 2), using the value $\xi_N(4.2\text{K}) = 0.06 \mu\text{m}$. There are no adjustable parameters. The good agreement between theory and data is remarkable, because previous experiments on SNS junctions have always yielded $I_C R_N$ values which were lower than theoretical predictions. In fact, the neglect of the proximity effect of the normal metal on the superconductor in the theory has led some workers to question the validity of the Likharev's result [15], although that theory is, at present, the only one which makes a prediction for the magnitude of $I_C R_N$. The results reported here are therefore very interesting, however more work is needed in order help resolve earlier differences between theory and experiment. Clearly studies of more samples having different dopings would be very useful; this work is in progress.

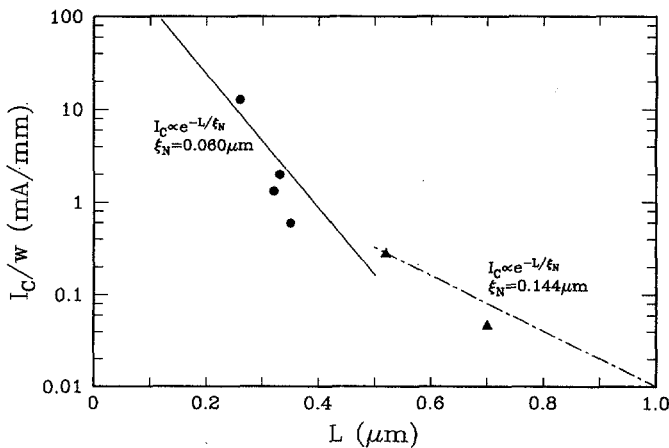


Figure 3: Critical current (normalized by device width) vs. measured link length for Nb/InAs/Nb weak link ($N_D = 3.5 \times 10^{17} \text{cm}^{-3}$). Solid circles are our data, triangles are from Ref. 8. The lines, of the form $\exp(-L/\xi_N)$, are drawn, using values for ξ_N appropriate for the two experiments, in order to illustrate consistency with the expected length dependence.

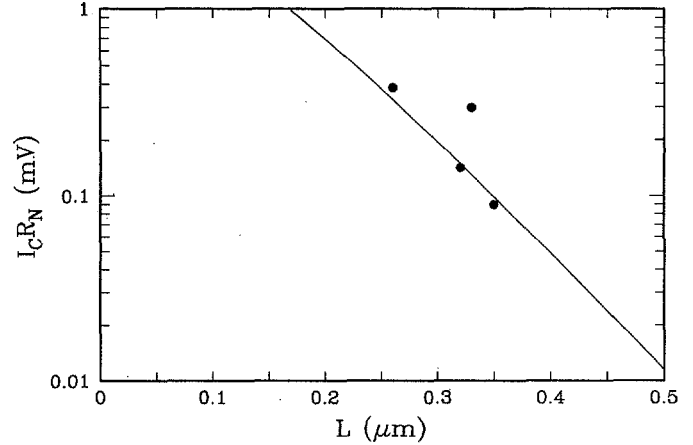


Figure 4: $I_C R_N$ product as a function of device length for our Josephson weak links (solid circles) and prediction of Likharev's theory [18] (solid line). The coherence length in the InAs is inferred from the temperature dependence of the critical current. There are no adjustable parameters.

Discussion

We have demonstrated SNS weak link devices on thin deposited InAs layers on GaAs substrates. The mobilities in these layers are somewhat lower than bulk values, however the normal metal coherence lengths in these layers are long enough that Josephson effects are observed in short ($0.26\text{-}0.35 \mu\text{m}$) Nb weak links fabricated on a layer having an electron concentration of $3.5 \times 10^{17} \text{cm}^{-3}$. Our results appear to be consistent with an earlier experiment on bulk InAs [9], which is to our knowledge the only other experiment in which semiconductor-coupled Josephson SNS (as opposed to SINIS) weak links were reported. Our structure has the advantage that device isolation is easily possible. These links, which are shorter than the earlier devices on bulk InAs, have $I_C R_N$ values as high as $380 \mu\text{V}$ (at 4.2 K), and which are in agreement with the theory of Likharev [17]. Such agreement has not been reported in earlier work on SNS weak links, and further experiments are in progress which are intended to further explore this issue.

The coherence length which we infer for our devices, $\xi_N(4.2\text{K}) = 0.060 \mu\text{m}$ gives an effective length (L/ξ_N) of 4.3 at 4.2 K for a $0.26 \mu\text{m}$ device. The sheet resistance of our layer is $360 \Omega/\square$, and could be increased through use of thinner layers. The use of a higher T_C electrode material would increase $I_C R_N$, but it would be desirable to decrease the effective device length, either by increasing ξ_N or decreasing the physical length. This would not only increase $I_C R_N$, but would also reduce its temperature and length dependences. For one of our more heavily-doped layers, $n = 3.1 \times 10^{19} \text{cm}^{-3}$ ($\mu = 1900 \text{cm}^2/\text{V-s}$), we expect a value of $0.16 \mu\text{m}$ for ξ_N and an effective length of 1.6 for a similar device at 4.2 K. The sheet resistance of this layer is only $10 \Omega/\square$, but the use of a 10 nm thick layer would raise it to $100 \Omega/\square$, so that a $1 \mu\text{m}$ wide device would have a resistance of 28Ω . These devices would already appear to be promising as Josephson weak links. However, it would be of interest to improve the mobility of the layers, or to work with two-dimensional electron gas structures, in order to achieve shorter effective device lengths.

Our structure is easily adapted to FET devices. The use of III-V heterostructures suggests superconducting MODFET and related structures. Clearly a major issue which needs attention is gate control of the resistance and critical current, an area in which the previously demonstrated SNS FETs performed poorly [12,13]

Semiconductor-coupled SNS weak links have considerable potential for use as Josephson devices and as the basis for superconducting FETs. Relatively little work has been done on these devices, which appear in these early experiments to behave in a similar fashion to conventional normal metal SNS weak links. This is in contrast to the many experiments on SINIS-type weak links, mostly using Si, which are not particularly well understood.

Acknowledgements

The authors wish to acknowledge the technical assistance of C. Jessen and G. Pepper in processing of the multilayers, and the services of J. Speidell,

who fabricated the masks for optical lithography. Partial support for this work was provided by the Office of Naval Research under contract N00014-85-C-0361.

References

1. K.K. Likharev, "Superconducting Weak Links", *Revs. Mod. Phys.* 51, 101 (1979).
2. M.R. Beasley, "Advanced Superconducting Materials for Electronic Applications", *IEEE Trans. Electron Dev.*, ED-27, 2009 (1980).
3. M.S. DiIorio and M.R. Beasley, "High T_C Superconducting Integrated Circuit: A dc SQUID with Input Coil", *IEEE Trans. Magnetics*, MAG-21, 532 (1985). H. Rogalla, B. David, M. Mück, and Y. Kato, "Study of Preparation Techniques for a Practical dc-SQUID Structure Fabricated from Nb_3Ge ", *IEEE Trans. Magnetics*, MAG-21, 536 (1985).
4. M. Schyfter, J. Maah-Sango, N. Raley, R. Ruby, B.T. Ulrich, and T. van Duzer, "Silicon Barrier Josephson Junctions in Coplanar and Sandwich Configurations", *IEEE Trans. Magnetics*, MAG-13, 862 (1977). R.C. Ruby and T. van Duzer, "Silicon-Coupled Josephson Junctions and Super-Schottky Diodes with Coplanar Electrodes", *IEEE Trans. Electron Dev.*, ED-28, 1394 (1981).
5. A. Serfaty, J. Aponte, and M. Octavio, "Properties of Step-Edge Pb-Si-Pb Josephson Junctions", *J. Low Temp. Phys* 63, 23 (1986).
6. T. Nishino, E. Yamada, and U. Kawabe, "Carrier Concentration Dependence of Critical Superconducting Current Induced by the Proximity Effect in Silicon", *Phys. Rev.* B33, 2042 (1986).
7. A.W. Kleinsasser, "Comment on 'Carrier Concentration Dependence of Critical Superconducting Current Induced by the Proximity Effect in Silicon'" (submitted to *Phys. Rev. B*).
8. M.F. Millea, A.H. Silver, and L.D. Flesner, "Superconducting Contacts to p-InAs", *IEEE Trans. Magnetics*, MAG-15, 435 (1979).
9. T. Kawakami and H. Takayanagi, "Single-Crystal n-InAs Coupled Josephson Junction", *Appl. Phys. Lett.* 46, 92 (1985).
10. A.H. Silver, A.B. Chase, M. McColl, and M.F. Millea, "Superconductor-Semiconductor Device Research", in *Future Trends in Superconductive Electronics*, B.S. Deaver, C.M. Falco, J.H. Harris, and S.A. Wolf, Eds., American Institute of Physics, New York, 1978, page 364.
11. T.D. Clark, R.J. Prance, and A.D.C. Grassie, "Feasibility of Hybrid Josephson Field Effect Transistors", *J. Appl. Phys.* 51, 2736(1980).
12. H. Takayanagi and T. Kawakami, "Superconducting Proximity Effect in the Native Inversion Layer on InAs", *Phys. Rev. Lett.* 54, 2449 (1985).
13. H. Takayanagi and T. Kawakami, "Planar-Type InAs-Coupled Three-Terminal Superconducting Devices", *Proc. Intl. Electron Devices Mtg.*, Washington, D.C., December, 1985.
14. T. Nishino, M. Miyake, Y. Harada, and U. Kawabe, "Three-Terminal Superconducting Device using a Si Single-Crystal Film", *IEEE Electron Dev. Lett.* EDL-6, 297 (1985).
15. R.B. van Dover, A. De Lozanne, and M.R. Beasley, "Superconductor-Normal-Superconductor Microbridges: Fabrication, Electrical Behavior, and Modeling", *J. Appl. Phys.* 52, 7327 (1981).
16. J. Seto and T. van Duzer, "Theory and Measurements on Lead-Tellurium-Lead Supercurrent Junctions", in *Proc. 13th Int'l. Conf. on Low Temp. Phys.*, Plenum, New York, 1972, Vol. 3, pg. 328.
17. K.K. Likharev, "The Relation $J_S(\phi)$ for SNS Bridges of Variable Thickness", *Pis'ma Zh. Tekh. Fiz.* 2, 29 (1976) [*Sov. Tech. Phys. Lett.* 2, 12, (1976)].
18. A.W. Kleinsasser, T.N. Jackson, G.D. Pettit, H. Schmid, J.M. Woodall, and D.P. Kern, "n-InAs/GaAs Heterostructure SNS Weak Links with Nb Electrodes" (submitted to *Appl. Phys. Lett.*).
19. S.M. Sze, *Physics of Semiconductor Devices*, Wiley, New York, 1981, Appendix G.